TECHNICAL ARTICLE

Experimental Characterization of Steel Fibre Knitted Fabrics Deformability

K. Vanclooster[1], M. Barburski[1,3], S.V. Lomov[1], I. Verpoest[1], F. Deridder[2], and F. Lanckmans[2]

1 Department MTM, KU Leuven, Leuven, Belgium
2 N.V. Bekaert S.A., Wetteren, Belgium
3 Institute of Architecture of Textile,Technical University of Lodz, Poland

Keywords
Deformability, Textile, Steel Fibres, Draping, Finite Elements

Correspondence
S.V. Lomov,
Department MTM,
KU Leuven,
Kasteelpark Arenberg 44 B-3001,
Leuven,
Belgium
Email: stepan.lomov@mtm.kuleuven.be

Received: March 28, 2012; accepted: November 27, 2012

doi:10.1111/ext.12009

Abstract

Extremely fine steel fibres (12 μm diameter) are spun into yarns and then knitted into fabric, which is used, among other applications, as a mould cover in forming of automotive glass. High requirements of the glass quality (absence of dioptric distortions) ask for a perfect evenness of the mould cover surface, which depends on the local distortions of the fabric, created during tensioning of the fabric over the mould. These distortions can be predicted using non-linear finite element draping simulation, providing that the material laws describing the fabric resistance to deformation are known. This article describes an experimental procedure for derivation of such laws using biaxial tension, shear, and compression tests. Test results for a typical steel fibre knitted fabric are presented together with an example of the draping simulation.

Introduction

Design and production of automobiles with more intricate and fantasy shapes and appearance, necessitate the usage of more sophisticated production methods for manufacturing of automobiles and their components. Car glasses influence the visibility of driver, must satisfy strict safety rules and also have significant effect on the car aesthetics. New shaping technologies allow applying complicated shapes with double curvature to smaller areas of glass.[1] In press bending, the glass sheet is first heated to temperatures of about 650°C and subsequently vacuum pressed on a steel mould. Direct contact between the steel mould and the glass would lead to inadmissible defects in the glass. To ensure the quality of the glass, a heat resistant separation material (HRSM) is used. In the past, ceramic paper separated the glass from a ceramic mould. Because of the brittleness of the ceramic the optical quality of the glass was often unsatisfactory. Nowadays, knitted steel fibre fabrics cover the mould which itself is made out of steel.[2] The knitted steel fibre fabrics come in direct contact with the glass and thus play a primary role in the quality of the formed glass, for example windshield.

During fabric mounting onto the mould (so-called ''draping''), tension variations occur across the fabric resulting in non-uniform deformation, which can change the evenness of the fabric thickness, local compression resistance, and smoothness of the fabric surface. This can have a serious impact on the quality of the glass. Draping simulation methods, well developed for garment design and forming of composite materials[3] can be used for design and optimisation of the fabric itself (yarn structure, knitting parameters etc...) and the tensions during mounting—providing that the deformation resistance laws of the material are known. These laws for steel fibre knitted fabrics have not been studied yet. Thus far, fabric manufacturers operate on the basis of empirical trial and error results to design their products. The challenge of this work is to establish an experimental procedure for identification of the material laws for steel fibre knitted fabric deformation resistance, and to use those experimental results to simulate the deformation behaviour of the fabric during mounting.

The methodology described here, whilst quite common for woven fabric used as composite reinforcements, was never applied to knitted fabrics, apart from scattered studies of specific deformation modes, for example, Refs. 4 and 5. This may be caused by a fact, that knitted fabrics are highly deformable, and do not cause problems when used as reinforced for composites (for example, helmets), and the fine details of their deformation do not affect the quality of the final product in such extent, as this happens in glass production. To the authors' knowledge, this is the first study of biaxial tension, shear, compression, and draping of knitted fabrics (be it steel, glass, or natural fibres) taken as a complex fabric characterization.

The tests described here were performed at the room temperature. This, of course, deviates from the actual high temperature environment during the glass forming. However, our aim was to establish the experimental technique for identification of the fabric behaviour during draping on the mould, which is done at room temperature. With this challenge met, high temperature behaviour of the fabric will be the subject of future research.

Material

The stainless steel fibres are obtained by a bundle drawing technique.[6,7] Metal wires form the starting material and are covered with a coating such as iron or copper. A bundle of these covered wires is subsequently enveloped in a metal pipe. Thereafter, thus the enveloped pipe is reduced in diameter via subsequent wire drawing steps alternated with an appropriate heat treatment to become a composite bundle with a smaller diameter. Inside the composite bundle, the initial wires have been transformed into thin fibres which are embedded separately in the matrix of the covering material. Such a bundle comprises between 500 and 1500 fibres. Once the desired final diameter has been obtained, the covering material is removed, for example, by solution in an adequate pickling agent or solvent. The final result is the naked fibre bundle. The fibres in the bundle are stretch-broken, and conventional spinning technologies are applied to produce a yarn. Figure 1 shows SEM images of a fibre, a yarn and a knitted fabric, as well as a photo of the fabric on a mould.

The steel (alloy 316L) is a common austenitic stainless steel (maximum 0.08% carbon, minimum 16% chromium, and sufficient nickel and/or manganese to retain an austenitic structure at all temperatures; molybdenum is added to improve corrosion resistance). Typical fibre diameter is 12 μm. The fibre is not circular and has rather hexagonal cross section, resulting from drawing of a highly compacted fibre bundle. Young modulus of the fibre is 170 GPa, ultimate elongation below 1%; tensile strength about 1800 MPa. The staple length of the fibres depends on the spinning technology (short or long staple) and ranges between 30 and 150 mm. The twist of double yarn is 130 turns/m ending with a yarn metric number ranging between 9/2 and 18/2 ($111 \times 2 - 55 \times 2$ tex) depending on the type of fabric. The yarns are ''hairy'' due to the stretch breaking. A knitted fabric is then made by weft knitting, normally on a circular knitting machine.

The fabric described in this article has the following parameters: areal density 950 g/m^2, yarn linear density 179 tex, number of loops per fabric width 1 loop/mm (knitting machine gauge 25). The knitted structure of the fabric defines two orthogonal principal directions: across the loops (''course'', denoted with subscript c) and along the loops (''wale'', denoted with subscript w).

Biaxial tension

Figure 2(a) shows the configuration of the biaxial tension test. A square fabric specimen (dimensions 270×270 mm) is clamped in a tensile machine with four independent arms, allowing simultaneous tension in course and wale direction with a given ratio of extension speeds (v_c,v_w) in two directions $k = v_c/v_w$, for $k =$ 1/0, 2/1, 1/1, 1/2, and 0/1. The maximum velocity in the pair (v_c,v_w) is 10 mm/min for all the tests. The clamp width is 200 mm. The rigid clamps are used. Segmented clamps were tried without success, as the fabric exhibit severe Poisson contraction near these clamps, disrupting the specimen configuration. The clamps are deliberately put as close one to another as possible. Use of a cross-shaped specimen leads to strong Poisson contraction of the arms. The fabric is pretensed with the force of 20 N, applied in the both directions; the value of pretension corresponds to the elimination of the initial fabric slack, which is determined by laser measurement of the position of the fabric surface. The strains in the middle of the specimen are measured optically using digital image correlation (DIC) technique (LIMESS system).[8] Because of changing texture of the fabric surface during deformation it was not possible to use the natural grey scale contrast of the fabric image to resolve displacement fields by full-field DIC. The DIC system registered displacement of a grid of points, marked on the fabric surface, and the average

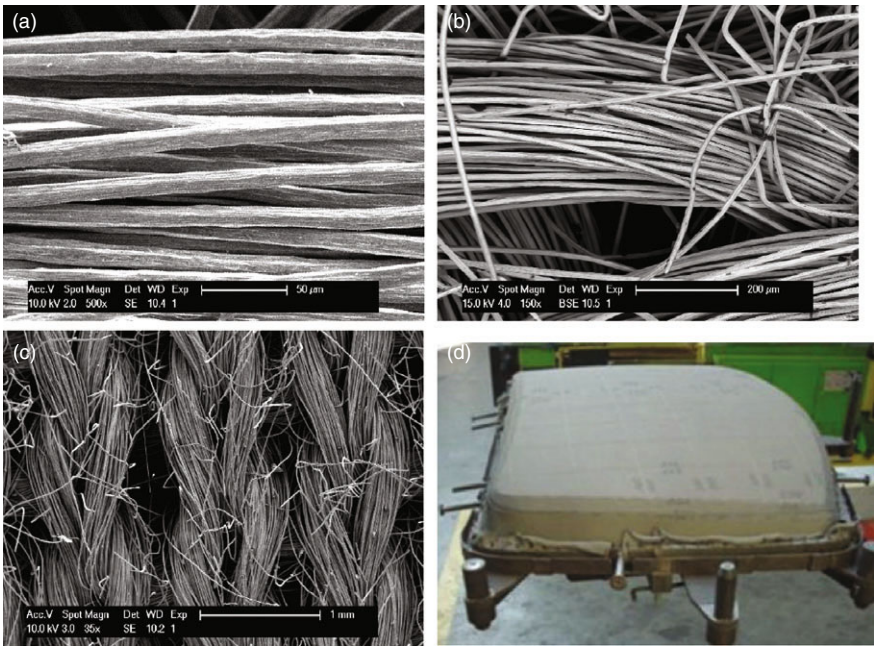

Figure 1 Steel fibre knitted fabric: (a) fibres in a yarn; (b, c) yarn loops in the fabric; and (d) the fabric on a mould.

surface strain was determined based on the measured displacements of these points. Figure 2(b) shows a typical result of the strain measurements. The scatter of strains in different points on the fabric surface is about 20%, hence, the strain field over the fabric surface is reasonably uniform.

The result of each test is dependency of the force per 1 mm of the clamped fabric width, applied in the course and wale directions on the average strain in the central part (120 × 120 mm) of the specimen. For any given k ratio four tests were done. In each test two force–strain dependencies are registered:

$$F_c = F_c(\varepsilon_c, \varepsilon_w|k); F_w = F_w(\varepsilon_c, \varepsilon_w|k) \quad (1)$$

where F_c and F_w are forces per unit length in the course and wale direction respectively, ε_c and ε_w are average deformations measured using DIC. Note that in these equations ε_c and ε_w are interdependent, as both curves are registered in the same test with the given k. Because of the difference between the deformations in the middle of specimen and the relative displacements of the grips, $\varepsilon_c/\varepsilon_w \neq k$ exactly (even if the ratio is close to the k value).

Dependency 1 combined for all the values of k, used in the test, allow derivation of a generic functions

$$F_c = F_c(\varepsilon_c, \varepsilon_w); F_w = F_w(\varepsilon_c, \varepsilon_w) \quad (2)$$

as interpolation of all the data points. The scatter of the points used for the least square interpolation is as follows: strains ε_c and ε_w at any given data point (determined by the global loading conditions) have a coefficient of variation (standard deviation to average ratio) of not more than 10%, force values of not more than 8%; each data point is the average result in four measurements.

Figure 2(c) illustrates the final result of the measurement: the material law, describing the fabric deformation resistance in in-plane biaxial tension (only the graph for the force in the course direction is shown). The response surfaces (2) are approximated with polynomial functions to be used in FE simulations. The range up to 20% deformation is the limit for the actual test configuration: at higher strains, the fabric starts being ruptured at the corners. This range is enough for representation of the actual draping process.

Shear: picture frame

During draping on a double-curvature mould (close to hemisphere; box shapes near corners etc.) a fabric shears. Shear leads to densification of the fabric fibrous structure, with possible ''locking'' leading to wrinkling, which is inadmissible for the glass forming. Shear deformation changes the local pattern of the knitted loops, with a potential imprint effects on the glass. Finally, the shear resistance, together with the tension forces, defines in-plane (''membrane'') deformation response of the fabric, and the material laws for these two types of deformation constitute the full system of equations necessary for finite element modelling of the draping.

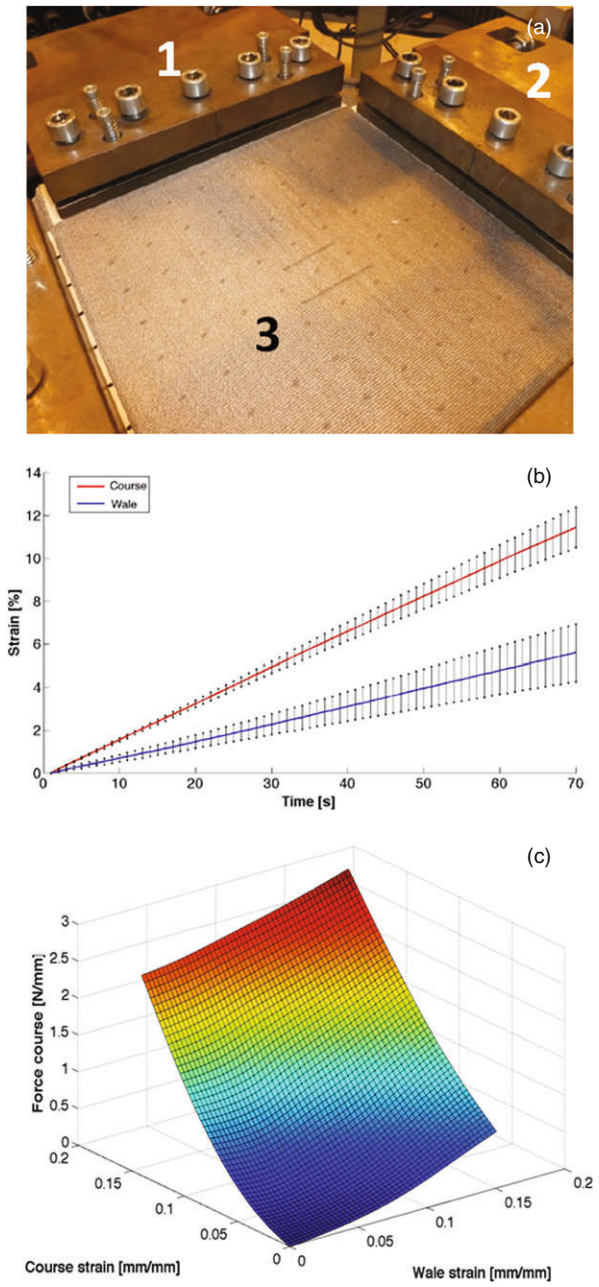

Figure 2 Biaxial arrangements and results: (a) biaxial tester: 1 and 2, moving clamps; 3, fabric specimen with painted dots for DIC deformation measurement; (b) $k = 0.5$, evolution of DIC-measured strains on the fabric: lines show average strains, error bars designate scatter of the strain in different points; and (c) biaxial test results: material law for in-plane tension.

Generally accepted device for measurement of shear deformation resistance of textile materials is so-called picture frame, shown in Fig. 3(a). A square fabric specimen is clamped in the frame, installed on a tensile machine. The course and wale directions are aligned with the frame sides, which initially are orthogonal. With the movement of the machine the frame, thanks for the hinged corners, imposes a shear deformation on the fabric. The speed of the tensile machine was 20 mm/min. As demonstrated in Refs. 9–11, the pretension of the fabric, created during its mounting on the frame, largely determines the shear resistance. Even simple mounting of a knitted fabric sample on the frame presents considerable difficulties due to rolling up of the fabric edges and slackness of the fabric. To avoid initial wrinkling of the heavy fabric, it is pretensed prior to the picture frame test on the biaxial tester with deformation 10% in the both directions; the fabric is fixed with a cardboard frame, taken off the biaxial tester and clamped in the picture frame; the cardboard is cut out (leftovers of the cardboard are seen in Fig. 3(a)). The shear angle of the fabric during the picture frame test normally well correspond to the kinematic shear angle of the frame[9,10]; however, this was checked using optical observations of the initially square grid drawn on the fabric (see Fig. 3(a)), and the difference between the shear angle determined kinematically and measured on the fabric was found to be below one. During the test a force–displacement curve is registered by the tensile machine. It is processed as follows: (1) the force-displacement registered in the test without fabric sample is subtracted to account for the frame weight and friction in hinges; (2) the displacement is transferred into shear angle using the kinematics of the frame; (3) tension force is transferred into shear force applied per unit width of the fabric. The reader is referred to Ref. 11 for the details of the data processing.

Three subsequent cycles of shear are registered. It is arguable which of the cycles should be taken as the fabric characterization. The reader is referred to Ref. 9 for the related discussion. We consider the first cycle that is considered as ''conditioning'' of the test setup, which relaxes tensions created by misalignments in the specimen mounting. The second and the third cycles are very close one to another, and the second cycle curve is taken for characterization. Tests with five fabric specimens are done, and the average of the five is taken as the final result of the test:

$$T = T(\gamma) \tag{3}$$

where T is the shear force per unit width, γ is the shear angle. The dependency 3 is illustrated in Fig. 3(b). The scatter in the values of the shear force for a given shear angle does not exceed 10% (coefficient of variation). The dependency 3 constitutes the material law, describing the fabric deformation resistance in in-plane shear.

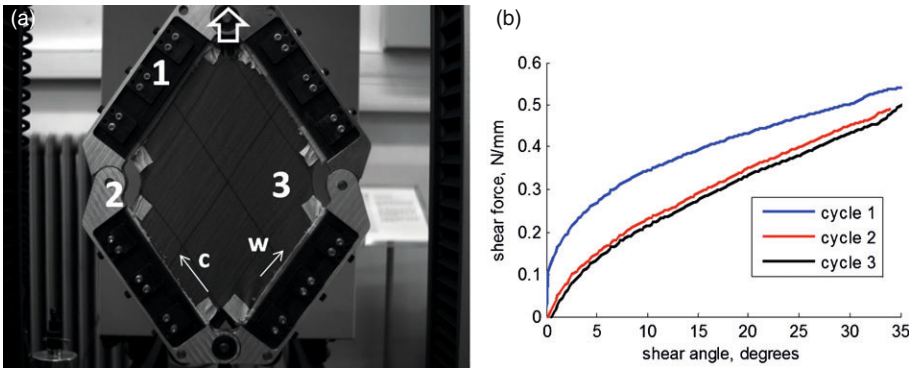

Figure 3 Picture frame test: (a) picture frame: 1, clamps; 2, hinges; 3, fabric specimen, the block arrow shows the upper hinge direction of movement, bottom hinge is stationary; thin arrows indicate the course and the wale directions; (b) shear test result: shear force–shear angle diagram, three loading cycles.

Compression

During vacuum glass forming the fabric, draped over the mould, undergoes through-the-thickness compression under a pressure of about 1 bar. As any fibrous/textile material, the fabric is highly compressible, and its thickness under 1 bar pressure can be 60–70% of the initial thickness. The compressibility theoretically changes with the local change of the fabric tension. The corresponding change of thickness may affect deviations of the local glass shape from the design surface, which may lead to unwanted optical distortions.

Figure 4(a) shows the arrangement of a compression test. Compression force was exerted on a fabric sample using a cylindrical head with the diameter of 70 mm. The fabric was placed on a spherical pivot; compression action without a sample was used to align the pivot to the compression head and to produce a ''calibration'' curve subtracted from the test force–displacement diagram to account for the machine compliance and to establish the zero thickness point. The test speed was 1 mm/min. The fabric was tested in the relaxed state and after pretension on the biaxial tester with prestrains of 5 × 5%, 10 × 10%, 0 × 10%, 10 × 0%, 0 × 20%, 20 × 0% (prestrain of 20 × 20% led to the fabric rupture).

The test results are expressed as fabric thickness—applied pressure diagrams (Fig. 4(b)). Three pressure cycles were done on each of the specimens and the third cycle was taken as the compression characteristic. Note that the first cycle is not representative because of the considerable fabric hairiness (see Fig. 1(c)). The second compression cycle was taken as characteristic of the fabric behaviour. The fabric undergoes several hundreds of compression acts during its life on the glass-forming mould. The tests with large number of cycles (up to 150) have shown that after the third cycle of compression the fabric thickness at 1 bar pressure changes not more than by 5%. The change of compression behaviour during cyclic loading can be characterised by the resilience coefficient (RC), which is the ratio between the area under the reloading compression curve to the area under loading compression curve. The *RC* values change with the cyclic loading as follows: 1st cycle 45%, 3rd cycle 83%, 10th cycle 86%, and 100th cycle 88%.

Figure 4(b) (insert) shows the difference of the fabric compressibility, expressed by the fabric thickness under 1 bar pressure, with the different tension conditions. With increase of the tension, the thickness can decrease by up to 70 μm or by about 12% of the relaxed fabric thickness. For thin glass, this difference can be significant for the glass optical properties.

The pressure–thickness relationship can be described using van Wyk formula[12]

$$t = t^* \left(\frac{p^*}{p} \right)^3 \tag{4}$$

where p is the pressure, t is the fabric thickness, $t*$ and $p*$ are parameters, identified by the least square fit to the experimental diagram in the pressure range from 5 to 100 kPa (practically important for vacuum forming). Equation 4 as such does not enter finite element calculations, but is used in post-processing to estimate the fabric thickness locally, under a given vacuum forming pressure and local deformation conditions.

Draping over a model mould and finite element simulations

Identification of the in-plane ''membrane'' material model (Eqs. 2 and 3) allows finite element modelling of the draping process (see Ref. 3 for a detailed description of draping simulations). The aim of such a simulation is determination, for certain loading scenario, the distribution of local tension and shear deformations. As described above, this information leads to estimations of the local distortions of the knitted pattern, identification of the loading scenarios

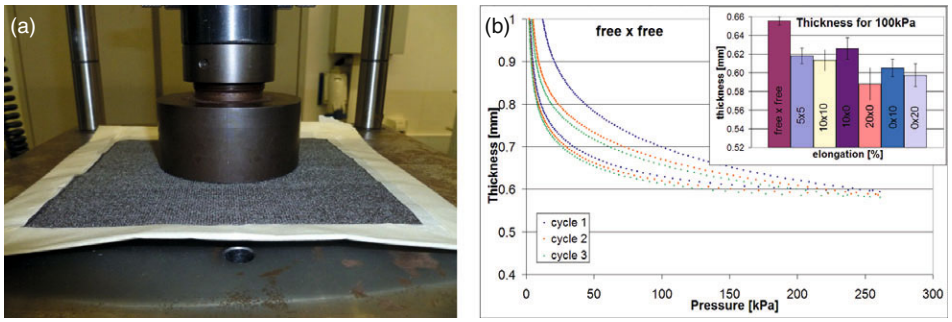

Figure 4 Compression test: (a) test arrangement; (b) thickness–pressure diagrams, three loading cycles; insert: fabric thickness under 1 bar pressure for different pretension.

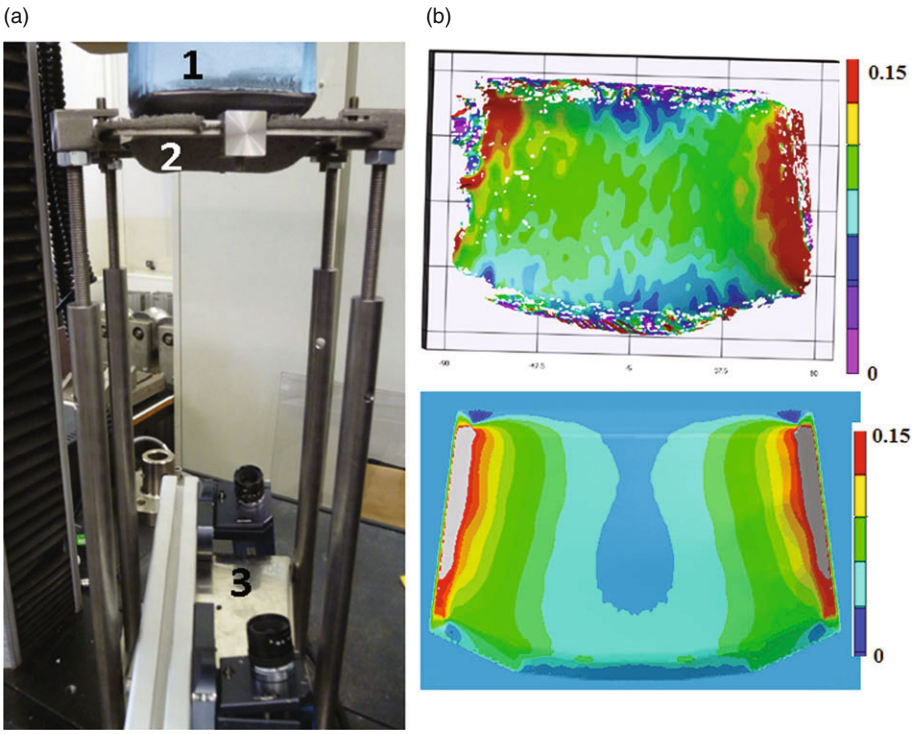

Figure 5 Draping experiment and FE simulation: (a) mould (1), fabric sample in the blankholder (2) on a mechanical testing machine with DIC cameras (3); (b) DIC registration (above) and FE simulation (below) of strains on the fabric surface, strain in horizontal (wale) direction.

which can lead to wrinkling or fabric rupture. Uniform distribution of deformation over the mould surface is a desirable feature of the production process. After validation of the draping simulations they can be used for optimisation of the loading scenario in a (future) automatisation of the draping.

Equations 2 and 3 offer themselves readily to be used in the draping simulation. However, it is important to remember that the tension and shear resistance was measured in macro-scale tests, whilst during FE simulation they are applied to micro-scale behaviour. Another deviation of a model, based on Eqs. 2 and 3 from reality may be in coupling of the tension and shear resistance,[13] which was not taken into account during the tests described below. Finally, numerical difficulties of the draping simulations cannot be underestimated: we deal with highly nonlinear behaviour of the material, with the presence of low stiffness deformation regimes, which may lead to numerical instabilities.

To validate the FE simulations, a test program on the draping of the fabric on a model mould was performed. Figure 5(a) shows the configuration of the test. The mould, made of hard foam, was punched on the fabric, tightly held by a blankholder (no slip boundary conditions were applied in the simulation). The deformed shape of the fabric was registered using DIC optical system with two cameras, which allow resolution of the full strain fields on the fabric surface.

The same deformation was modelled in FE ABAQUS package, using explicit simulations. The user defined material routines (UMAT), implementing the material laws (2) and (3), and objective differentiation for large fabric deformations[14] were used. The reader is referred to Ref. 15 for details of the UMAT implementation.

The results of the experimental registration of the strains and FE simulations are compared in Fig. 5(b). The simulations correctly predict the strain distribution over the mould. For the central area of the mould (defined by its rounded edges) the maximum strain in the wale direction is predicted as 9.8%, experimental value is 9.0%; for the course direction the predicted maximum strain is 18%, measured 19%. These results show that the model correctly describes the deformation behaviour and correctly estimates the distribution of strains over the mould—the parameter most important for the practical optimisation of the draping process. However, the reaction force is predicted with a large error (several times), which can be attributed to the fact that in the identification of the material resistance parameters pretension was used both for biaxial tension and shear. The actual boundary conditions in the draping experiment (blankholder force governed by friction) are difficult to identify, as well as a difficult-controlled slack of the fabric. In spite of these difficulties, adequacy of the simulations is supported by the fact that the ranging of resistance of different fabrics is correctly represented in the simulations.

Conclusions

An experimental procedure is proposed for study of deformation resistance of weft-knitted steel fibre fabrics, used as separation layer in glass forming. The procedure includes biaxial tension, shear (picture frame), and compression tests. The experimental procedure has been validated as a tool for identification of material laws, necessary for finite element draping simulations, which will lead to optimisation of loading scenarios for the cloth draping during for the mould preparation in the glass forming process.

Acknowledgments

The work was funded by IWT (Flanders), project IWT/090336 and by the grant 631/MOB/2011 of the Polish Ministry of Science and High Education (MB), with the support from N.V. Beckaert S.A. The help of technicians of the Department MTM, KU Leuven—Bart Pelgrims and Kris Van de Staey—is gratefully acknowledged.

References

1. Griffiths, J., ''Glass Act [Glass in Automotive Design],'' *Automotive engineer* **31**(8):35 (2006).
2. Van Steenlandt, W., and Heirbaut, G., *Reinforced Knitted Structure Comprising Metal Fibres* (2002) US patent 6407016.
3. Boisse, P., (ed.), *Composite Reinforcements for Optimum Performance*, Woodhead Publishing: Oxford (2011).
4. Lomov, S.V., Moesen, M., Stalmans, R., Trzcinski, G., Van Humbeek, J., and Verpoest, I., Finite Element Modelling of SMA Textiles: Superelastic Behaviour. *Journal of the Textile Institute* **102**(3): 232–247 (2011).
5. Boisse, P., Gasser, A., Hagege, B., and Billoet, J.-L., ''Analysis of the Mechanical Behavior of Woven Fibrous Material Using Virtual Tests at the Unit Cell Level,'' *Journal of Material Science* **40**:5955–5962 (2005).
6. Webber, H.H., and Winson, A.H., *Method of Simultaneously Forming a Plurality of Filaments* (1965) US patent 3277564.
7. Roberts, J.A., and Roberts, P.R., *Method of Forming Filaments* (1968) US patent 3394213.
8. Lomov, S.V., Boisse, P., Deluycker, E., et al., ''Full Field Strain Measurements in Textile Deformability Studies,'' *Composites Part A* **39**:1232–1244 (2008).
9. Lomov, S.V., Willems, A., Verpoest, I., Zhu, Y., Barburski, M., and Stoilova, T., ''Picture Frame Test of Woven Fabrics with a Full-Field Strain Registration,'' *Textile Research Journal* **76**(3):243–252 (2006).
10. Lomov, S.V., Ivanov, D.S., Verpoest, I., et al., ''Full Field Strain Measurements for Validation of Meso-FE Analysis of Textile Composites,'' *Composites Part A* **39**:1218–1231 (2008).
11. Cao, J., Akkerman, R., Boisse, P., et al., ''Characterization of Mechanical Behavior of Woven Fabrics: Experimental Methods and Benchmark Results,'' *Composites Part A* **39**:1037–1053 (2008).
12. Van Wyk, C.M., ''Note on the Compressibility of Wool,'' *Journal of the Textile Institute* **37**:T285–T292 (1946).
13. Harrison, P., Abdiwi, F., Guo, Z., Potluri, P., and Yu, W.R., ''Characterising the Shear-Tension Coupling and Wrinkling Behaviour of Woven Engineering Fabrics,'' *Composites Part A* **43**:903–914 (2012).
14. Willems, A., Lomov, S.V., Verpoest, I., Vandepitte, D., Harrison, P., and Yu, W.R., ''Forming Simulation of a Thermoplastic Commingled Woven Textile on a Double Dome,'' *11th ESAFORM2008 Conference on Material Forming*, Lyon (2008).
15. Willems, A., *Forming Simulation of Textile Reinforced Composite Shell Structures*, PhD Thesis, Department MTM, Katholieke Universiteit Leuven (2008).